

# Are the nearby groups of galaxies gravitationally bound objects?

Sami-Matias Niemi,<sup>★</sup> Pasi Nurmi,<sup>★</sup> Pekka Heinämäki<sup>★</sup> and Mauri Valtonen<sup>★</sup>

*University of Turku, Tuorla Observatory, Väisäläntie 20, Piikkiö, Finland*

Accepted 2007 September 19. Received 2007 September 19; in original form 2007 April 2

## ABSTRACT

We have compared numerical simulations to observations for the nearby ( $<40$  Mpc) groups of galaxies. The group identification is carried out using a group-finding algorithm developed by Huchra & Geller. Using cosmological  $N$ -body simulation code with the  $\Lambda$  cold dark matter ( $\Lambda$ CDM) cosmology, we show that the dynamical properties of groups of galaxies identified from the simulation data are, in general, in a moderate, within  $2\sigma$ , agreement with the observational catalogues of groups of galaxies. As simulations offer more dynamical information than observations, we used the  $N$ -body simulation data to calculate whether the nearby groups of galaxies are gravitationally bound objects by using their virial ratio. We show that in a  $\Lambda$ CDM cosmology about 20 per cent of nearby groups of galaxies, identified by the same algorithm as in the case of observations, are not bound, but merely groups in a visual sense. This is quite significant, specifically because estimations of group masses in observations are often based on an assumption that groups of galaxies found by the friends-of-friends algorithm are gravitationally bound objects. Simulations with different resolutions show the same results. We also show how the fraction of gravitationally unbound groups varies when the apparent magnitude limit of the sample and the value of the cosmological constant  $\Lambda$  is changed. In general, a larger value of the  $\Omega_\Lambda$  generates slightly more unbound groups.

**Key words:** methods: numerical – galaxies: clusters: general – galaxies: haloes – dark matter – large-scale structure of Universe.

## 1 INTRODUCTION

Small groups of galaxies are the most common galaxy associations and contain  $\sim 50$  per cent of all galaxies in the Universe (e.g. Holmberg 1950; Humason, Mayall & Sandage 1956; Huchra & Geller 1982; Geller & Huchra 1983; Nolthenius & White 1987). The study of galaxy groups is a very interesting area of research because these density fluctuations lie between galaxies and clusters of galaxies, and may provide important clues to galaxy formation. Small groups of galaxies are also important cosmological indicators of the distribution, and properties, of dark matter in the universe.

The dynamics of the nearby groups of galaxies and the Local Group has provided a unique challenge to cosmological models in the past. The quiescence of the local peculiar velocity field (e.g. de Vaucouleurs 1958; Sandage & Tammann 1975; Sandage 1999; Ekholm et al. 2001) was a long-standing puzzle that presented a challenge for the models of structure formation. The velocity field within  $5 h^{-1}$  Mpc of the Local Group is extremely ‘cold’, the dispersion is only  $\sim 50$ – $60$  km s $^{-1}$  (Teerikorpi, Chernin & Baryshev 2005, and references therein). The  $\Lambda$ CDM cosmology and dark energy have solved this problem and it has been shown by, for example,

Klypin et al. (2003), Macció, Governato & Horellou (2005) and Peirani & de Freitas Pacheco (2006) with constrained simulations that the  $\Lambda$ CDM cosmology can produce the small values of the velocity dispersion. Today, the question of the virialization of groups of galaxies and the fraction of gravitationally bound systems provides a new challenge for the cosmological models and grouping algorithms.

Over the last two decades, cosmological simulations have proven to be an invaluable tool in testing theoretical models in the non-linear regime. The standard approach is to assume a cosmological model and to use the appropriate power spectrum of the primordial perturbations to construct a random realization of the density field within a given simulation volume. The evolution of the initial density field is then followed by using an  $N$ -body simulation code, and the results in the simulation box (viewed from outside) are compared with observational data. A comparison of the simulations with observational data is typically done in a statistical manner. The statistical approach works well if there is a statistically representative sample of objects with well-understood selection effects for both the observed universe and the simulations.

Given a set of observed galaxies with their positions in the sky and their redshifts, the task of a group finder is to return sets of galaxies that most likely represent true gravitationally bound structures. Some contamination is always expected due to selection effects in observations. This study uses one of the most popular group finders:

<sup>★</sup>E-mail: saniem@utu.fi (SMN); pasnurmi@utu.fi (PN); pekheina@utu.fi (PH); mvaltonen2001@yahoo.com (MV)

the friends-of-friends (FOF) algorithm. FOF has been used widely for identifying groups of galaxies in the redshift surveys (Huchra & Geller 1982; Geller & Huchra 1983; Nolthenius & White 1987; Ramella, Geller & Huchra 1989; Moore, Frenk & White 1993; Ramella, Pisani & Geller 1997; Giuricin et al. 2000; Tucker et al. 2000; Ramella et al. 2002) and is now a standard approach.

The identification of the group members has, in general, been based on a subjective selection of data. In order to remove this difficulty, Huchra & Geller (1982, hereafter HG82) developed a method of identifying groups of galaxies from the observations. It has been usually thought that the FOF based algorithms would produce groupings which are mostly gravitationally bound when the number of galaxies in a group exceeds five members (see e.g. Ramella et al. 2002). A few studies (e.g. Carlberg et al. 2001) have been made where the free parameters of the FOF algorithm have been optimized to avoid spurious groups with interlopers. Studies of the FOF algorithms have concluded that the choice of the free parameters depends on the case that is studied, and no singular best choice of the parameters can be made. Unfortunately, none of the observational methods do truly answer the question whether groups of galaxies are gravitationally bound objects. There are some estimates for the fraction of how many groups found by the FOF algorithm are spurious (see e.g. Ramella et al. 2002), but these estimates are not based on the physical properties of the groups.

Cosmological  $N$ -body simulations include all the necessary information for finding out whether a given object is gravitationally bound or not. Aceves & Velázquez (2002) studied small galaxy groups with  $N$ -body simulations and made conclusions about the virialization of the groups. Diaferio, Geller & Ramella (1994) studied compact groups of galaxies with  $N$ -body simulations and made remarks about the fraction of bound groups and chance alignment systems. Groups of galaxies, and their dynamical properties generated by the FOF algorithm, have been studied earlier with  $N$ -body simulations (see e.g. Nolthenius, Klypin & Primack 1997; Diaferio et al. 1999; Merchán & Zandivarez 2002; Casagrande & Diaferio 2006). Most of these earlier studies have taken advantage of the constrained simulations and have used models which are different from the currently popular  $\Lambda$ CDM cosmology. In these constrained, or mock catalogue, simulations, the simulated space has been compared directly with the observations of redshift space and the groups have been categorized as spurious if the algorithm has failed to find similar groups as in real space. Instead, we have studied the virial ratio of the groups of galaxies produced by the FOF algorithm first described in HG82. We will show that  $\sim 20$  per cent of the groups of galaxies found by the FOF algorithm are not real gravitationally bound groups, but spurious. Our results agree roughly with the previous results and estimates but do not confirm the claim by Ramella et al. (1989) that groups with more than four members are gravitationally bound.

For an ‘observer’ placed in a specific location, selecting a similar environment between observational data and cosmological simulations might be problematic. The simplest way is to choose an ‘observation’ point within a simulation box by certain criteria. It is argued (e.g. Klypin et al. 2003, and references therein) that it is not clear what ‘similar environment’ actually means and that simply placing the observer at some specific point would resolve the issue. In this paper, we show that this is a useful approach, as we are not comparing simulations to observations directly but with statistics.

The main purpose of this work is to study if groups of galaxies found by the HG82 algorithm are bound, and how the fraction of bound groups depend on the chosen magnitude limit and cosmological model. We will show our findings with different apparent

magnitude limits and for different cosmological models. We also show that there is no significant correlation between the crossing time of a group and its virial ratio.

This paper is organized as follows. In Section 2, we review the method used in the identification of the group members in the observations. A brief discussion of the differences between observations and simulations is given in Section 2. In Section 3, we discuss briefly the virial ratio, used for determining whether a group of galaxies is gravitationally bound. Section 4 discusses the simulations, we use for the analysis. In Sections 5 and 6, we present our results and discuss the findings. Discussion of the probability functions of gravitationally unbound groups is done in Section 7. Finally, we summarize our results in Section 8.

## 2 A REVIEW OF THE GROUP-FINDING ALGORITHM

In observations, there are generally three basic pieces of information available for the study of the galaxy distribution: the position, the magnitude and the redshift of each galaxy. Although the magnitude is important as a measure of the object’s visibility, it is usually a poor criterion for group membership. The method used for creating a group catalogue in HG82 can be summed up in two criteria: the projected separation and the velocity difference. The FOF algorithm is described in greater detail by the original authors in HG82.

The grouping method begins with a selection of an object, which has not been previously assigned to any of the existing groups. After choosing the object, the next step is to search for companions with the projected separation  $D_{12}$  smaller or equal to the separation  $D_L$ :

$$D_{12} = 2 \sin\left(\frac{\theta}{2}\right) \frac{V}{H_0} \leq D_L(V_1, V_2, m_1, m_2), \quad (1)$$

where the mean cosmological expansion velocity is

$$V = \frac{V_1 + V_2}{2}, \quad (2)$$

and the velocity difference  $V_{12}$  is smaller or equal to the velocity  $V_L$ :

$$V_{12} = |V_1 - V_2| \leq V_L(V_1, V_2, m_1, m_2), \quad (3)$$

where  $V_1$  and  $V_2$  refer to the velocities (redshifts) of the galaxy and its companion,  $m_1$  and  $m_2$  are their magnitudes and  $\theta$  is their angular separation in the sky. If no companions are found, the galaxy is entered in a list of isolated galaxies. All companions found are added to the list of group members. The surroundings of each companion are then searched by using the same method used in the first place to find companions. This process is repeated until no further members are found.

There are a variety of prescriptions for  $D_L$  and  $V_L$ . We adopt the method used in HG82, and assume that the luminosity function is independent of distance and position and that at larger distances only the fainter galaxies are missing. For each pair we take

$$D_L = D_0 \left[ \frac{\int_{-\infty}^{M_{12}} \Phi(M) dM}{\int_{-\infty}^{M_{lim}} \Phi(M) dM} \right]^{-1/3}, \quad (4)$$

where the integration limits can be calculated from equations:

$$M_{lim} = m_{lim} - 25 - 5 \log(D_F) \quad (5)$$

and

$$M_{12} = m_{lim} - 25 - 5 \log(V), \quad (6)$$

and where  $\Phi(M)$  is the differential galaxy luminosity function for the sample and  $D_0$  is the projected separation in Mpc chosen at some fiducial distance  $D_F$ . In this paper, we adopt constants  $D_0 = 0.63$  Mpc and  $D_F = 10$  Mpc to be same as in HG82. The effect of varying  $D_0$  has been studied, for example, by Ramella et al. (1989) where the effects are also explained.

The limiting velocity difference is scaled in the same way as the distance  $D_L$ :

$$V_L = V_0 \left[ \frac{\int_{-\infty}^{M_{12}} \Phi(M) dM}{\int_{-\infty}^{M_{\text{lim}}} \Phi(M) dM} \right]^{-1/3}, \quad (7)$$

where the fiducial value is  $V_0 = 400 \text{ km s}^{-1}$  and the integration limits are as above (equations 5 and 6). Ramella et al. (1989) varied  $V_0$  and concluded that the results are not sensitive to the choice of  $V_0$ . This is probably related to the geometry of the large-scale structure. Frederic (1995a,b) argues that the optimal choice of  $D_0$  and  $V_0$  depends on the purpose for which groups are being identified. Similar claims has been made in papers where the FOF algorithm has been optimized (see e.g. Eke et al. 2004; Berlind et al. 2006). Because of this, we also show some results when  $D_0 = 0.37$  Mpc and  $V_0 = 200 \text{ km s}^{-1}$  are adopted.

Note that the scaling law in equations (4) and (7) has been questioned by many authors. Specifically, replacing the power  $-1/3$  by  $-1/2$  (see the argument in e.g. Nolthenius & White 1987; Gourgoulhon, Chamaroux & Fouqué 1992) drastically reduces the correlation between the redshift and the velocity dispersion observed in the HG82 group catalogue. However, part of this correlation is related to a selection effect rather than to the grouping algorithm, because groups with low-velocity dispersion usually have few bright galaxies and so they can be seen only at low redshift. In this paper, we use the equations mentioned above for consistency with the HG82 catalogue.

For simplicity, we use the Schechter (1974) luminosity function:

$$\Phi(M) = \frac{2}{5} \Phi^* \ln 10 \left[ 10^{2/5(M^* - M)} \right]^{\alpha+1} \exp^{-10^{2/5(M^* - M)}}, \quad (8)$$

where  $M$  is the absolute magnitude of the object. We adopt the parameter values of  $\alpha = -1.02$ ,  $M^* = -19.06$  and  $\Phi^* = 0.0277$  comparable to HG82. For comparison, we use the galaxy luminosity function values of  $\alpha = -1.15$ ,  $M^* = -19.84$  and  $\Phi^* = 0.0172$ , which were derived from the Millennium Galaxy Catalogue by Driver et al. (2007).

Our chosen values of constants and parameters needed for the FOF algorithm are exactly the same as in HG82 for consistency. We do show selected results with more recent values of constants and parameters if these results differ from the results produced with the HG82 values. Throughout this paper, we adopt the parametrized Hubble constant  $H_0 = 100 h \text{ km s}^{-1} \text{ Mpc}^{-1}$  with  $h = 1.0$  for comparison with HG82 when a definite value of the Hubble constant is needed. We do not consider dust extinction in the analysis of the simulations in this paper.

### 3 A REVIEW OF THE VIRIAL THEOREM

In the simplest case, when we have a two body system with total mass  $M = m_1 + m_2$  and  $V$  is the relative speed of the components, the kinetic energy is  $T$  of the system (in the centre-of-mass coordinate system) and its gravitational potential energy  $U$  (taken positive) are:

$$T = \frac{1}{2} \frac{m_1 m_2}{M} V^2, \quad (9)$$

$$U = \frac{G m_1 m_2}{R}, \quad (10)$$

where  $R$  is the size of the system and  $G$  is the gravitational constant. These equations are related by a simple relation:

$$U = 2T. \quad (11)$$

However, the above relation holds only for isolated self-gravitating systems when the system is in equilibrium.

In general, groups of galaxies (and dark matter haloes<sup>1</sup>) contain more than two members. Therefore, a generalized method for calculating the kinetic and the potential energies is needed. We adopt a method described by Chernin & Mikkola (1991). In general, the kinetic energy may be written as

$$T = \frac{1}{2M} \sum_{i < j} m_i m_j (\mathbf{V}_i - \mathbf{V}_j)^2, \quad (12)$$

and the potential energy as

$$U = G \sum_{i < j} \frac{m_i m_j}{R_{i,j}}, \quad (13)$$

where  $m_i$  and  $m_j$  are the masses of the two galaxies,  $\mathbf{V}_i$  and  $\mathbf{V}_j$  are their velocities and  $R_{i,j}$  is the distance between them.

We use these general equations to get the total kinetic energy of a group of haloes and compare it to its total potential energy. If the group of haloes does not fulfill the criterion:

$$T - U < 0, \quad (14)$$

it is entered into a list of unbound groups. The above criterion is equal to the virial ratio:

$$\frac{T}{U} < 1.0, \quad (15)$$

which we use throughout this paper as a criterion for discriminating between bound and unbound groups.

## 4 DESCRIPTION OF THE COSMOLOGICAL SIMULATIONS

### 4.1 Background

We present results from four simulations, performed by the cosmological  $N$ -body simulation code Adaptive Mesh Investigations of Galaxy Assembly (AMIGA). The former version of AMIGA was known as MLAPM (for details see Knebe, Green & Binney 2001). For the first two runs, we adopt the currently popular flat low-density cosmological model  $\Lambda$ CDM with  $h = 1.0$ ,  $\Omega_{\text{dm}} = 0.27$ ,  $\Omega_{\Lambda} = 0.73$  and  $\sigma_8 = 0.83$ , with two different resolutions. Both simulations were made with  $256^3$  dark matter particles. The high-resolution simulation began at the initial redshift of  $z_i = 47.96$  while the low-resolution simulation was initiated at redshift  $z_i = 38.71$ . The volume employed in the high-resolution simulation was  $(40 h^{-1} \text{ Mpc})^3$  and  $(80 h^{-1} \text{ Mpc})^3$  in the low-resolution simulation corresponding to the mass resolutions of  $2.86 \times 10^8$  and  $2.29 \times 10^9 h^{-1} M_{\odot}$ , respectively. The force resolution for the high-resolution simulation is  $1.8 h^{-1} \text{ kpc}$  and for the low resolution  $7.3 h^{-1} \text{ kpc}$ .

For the third and the fourth simulations, we adopt different cosmological models. These simulations were also performed with  $256^3$

<sup>1</sup> We will use the term ‘halo’ from now on to refer to virialized clumps of dark matter in the simulation and reserve ‘galaxy’ for the real observational data.

**Table 1.** Details of the simulations analysed in this paper.

$\Omega_\Lambda$	$L$	$N_p$	$z_i$	$m_{\text{res}}$	$F_{\text{res}}$	$N_h$
0.73	40	$256^3$	47.9600	$2.86 \times 10^8$	1.8	6700
0.73	80	$256^3$	38.7099	$2.29 \times 10^9$	7.3	9301
0.90	80	$256^3$	31.7858	$8.50 \times 10^8$	7.3	4937
0.00	80	$256^3$	72.8767	$8.47 \times 10^9$	3.7	7919

Note:  $\Omega_\Lambda$  specifies the value of the cosmological constant,  $L$  is the size of the simulation box in one dimension in  $h^{-1}$  Mpc,  $N_p$  is the number of dark matter particles,  $z_i$  is the initial redshift,  $m_{\text{res}}$  is the mass resolution in  $h^{-1} M_\odot$ ,  $F_{\text{res}}$  is the force resolution in  $h^{-1}$  kpc and  $N_h$  is the total number of dark matter haloes identified from the simulation.

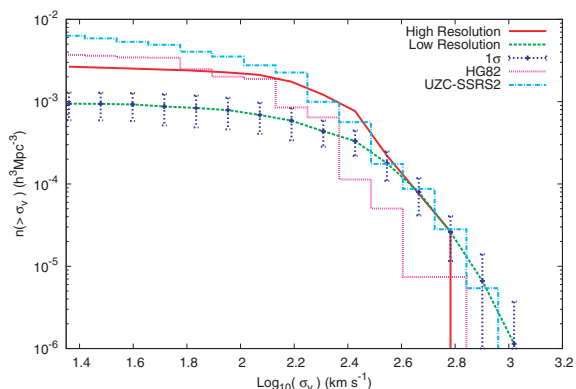


**Figure 1.** The cumulative number density of velocity dispersion  $\sigma_v$  for galaxy groups. Simulation data are from the  $\Omega_\Lambda = 0.73$  simulations, and it is averaged over the ensemble of 10 mock catalogues. The error bars are  $1\sigma$  errors and are only shown for the low-resolution  $\Omega_\Lambda = 0.73$  simulation for clarity. The error bars for other data have similar size.

dark matter particles but with different values of the cosmological constant  $\Lambda$ . The total density of the universe was kept equal to the critical density ( $\Omega = 1.0$ ). For the third simulation, we adopt  $h = 1.0$ ,  $\Omega_{\text{dm}} = 0.1$ ,  $\Omega_\Lambda = 0.9$  and  $\sigma_8 = 0.83$ . For the fourth simulation, we adopt  $h = 1.0$ ,  $\Omega_{\text{dm}} = 1.0$ ,  $\Omega_\Lambda = 0.0$  and  $\sigma_8 = 0.84$  (see Table 1).

The high-resolution  $\Omega_\Lambda = 0.73$  simulation was used to understand the effects of limited resolution in  $N$ -body simulations. During this work, we found some differences between results of the high- and the low-resolution  $\Omega_\Lambda = 0.73$  simulations. These differences are clearly visible when the group abundances are studied (see Figs 1–4).

#### 4.2 Halo finder and identification of the dark matter haloes

Our simulations only follow the evolution of the dark matter particles via gravitational interaction. It is expected that baryons condense and form galaxies at the centres of dark matter haloes. AMIGA  $N$ -body simulation code comes with a halo-finding algorithm called MHF (MLAPM’s Halo Finder, Gill, Knebe & Gibson 2004). For our purpose of analysing the nearby groups of haloes we used MHF.

The general goal of a halo finder, such as MHF, is to identify gravitationally bound objects. MHF essentially uses the adaptive grids of the AMIGA to locate the haloes and the satellites of the host haloes, namely subhaloes. The advantage of reconstructing the grids to locate haloes is that they follow the density field with the exact accuracy of the simulation code and therefore no scaling length is

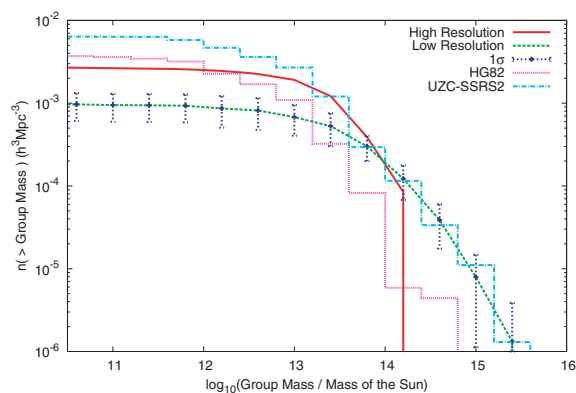


**Figure 2.** Group abundance by ‘observable’ mass of the groups. Simulation data are from the  $\Omega_\Lambda = 0.73$  simulations, and it is averaged over the ensemble of 10 mock catalogues. The error bars are  $1\sigma$  errors and are only shown for the low-resolution  $\Omega_\Lambda = 0.73$  simulation for clarity. The error bars for other data have similar size.

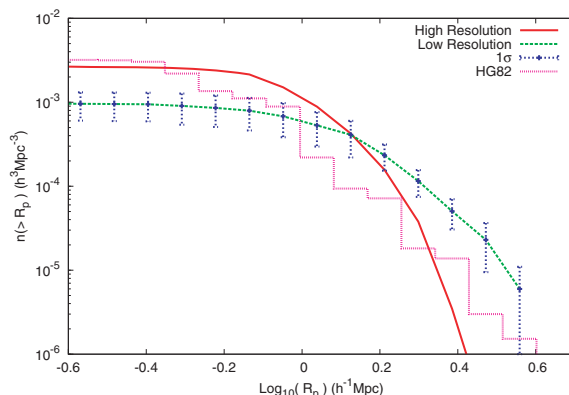


**Figure 3.** The cumulative distribution of mean pairwise separation  $R_p$  for galaxy groups. Simulation data are from the  $\Omega_\Lambda = 0.73$  simulations, and it is averaged over the ensemble of 10 mock catalogues. The error bars are  $1\sigma$  errors and are only shown for the low-resolution  $\Omega_\Lambda = 0.73$  simulation for clarity. The error bars for other data have similar size.

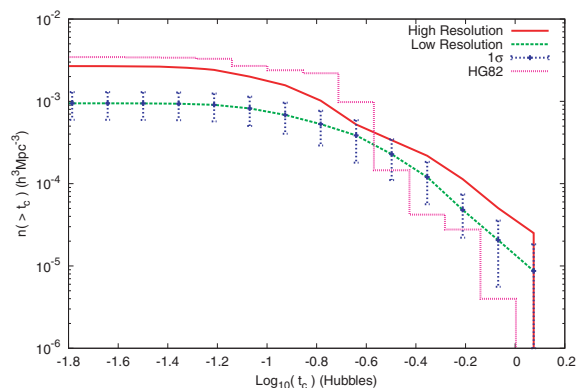


**Figure 4.** The cumulative distribution of crossing time  $t_c$  (in unit of the Hubble time) for galaxy groups. Simulation data are from the  $\Omega_\Lambda = 0.73$  simulations, and it is averaged over the ensemble of 10 mock catalogues. The error bars are  $1\sigma$  errors and are only shown for the low-resolution  $\Omega_\Lambda = 0.73$  simulation for clarity. The error bars for other data have similar size.

required [for more detailed description of the MHF see Gill et al. (2004)].

The minimum number of particles in a halo was set to 10. This corresponds to a halo mass  $\sim 3 \times 10^9$  and  $\sim 2 \times 10^{10} h^{-1} M_\odot$  for the high- and the low-resolution simulation, respectively. A low value of the minimum number of particles in a halo ensures that even with a limited resolution, large and massive haloes are split into lighter subhaloes. For large and massive ( $\sim 10^{14} h^{-1} M_\odot$ ) haloes, subhaloes represent visual galaxies, masses  $\sim 10^{12} h^{-1} M_\odot$ . In a typical case, the total mass fraction in subhaloes is  $\sim 10$  per cent, and only these are visible in our ‘mock’ catalogue. In our ‘mock’ catalogue, the median of individual dark matter haloes mass is  $\sim 1.6 \times 10^{12} h^{-1} M_\odot$  when the  $\Omega_\Lambda = 0.73$  model and the low resolution is adopted. The first and the third quartiles are:  $\sim 7.2 \times 10^{11}$  and  $\sim 5.0 \times 10^{12} h^{-1} M_\odot$ , respectively.

The AMIGA and its halo finder calculate automatically certain properties (e.g. position, mass, velocity, etc.) of the dark matter haloes. These properties were used when the FOF algorithm was applied to generate the catalogues of groups of dark matter haloes. Subhaloes were included in our data as our purpose is to study if the groups of galaxies (dark matter haloes) are gravitationally bound objects. The results did not change substantially when the subhaloes of the more massive haloes were excluded from the analysis. This result is due to the small number of subhaloes in our low-resolution simulation. The results of the high-resolution simulation show no significant difference if subhaloes were excluded because subhaloes have a relatively small mass. Due to their small masses, subhaloes are not visible at the observation point, when the apparent magnitude limit of 13.2 is adopted.

## 5 STATISTICAL PROPERTIES OF THE NEARBY GROUPS OF GALAXIES: COMPARING SIMULATIONS WITH OBSERVATIONS

### 5.1 Selection of the nearby groups of haloes

A Total of 10 catalogues were generated, corresponding to 10 different ‘observers’, for each simulation, with different apparent magnitude limits. 10 observers are used to produce enough groups to give good statistics. Note, however, that since all 10 catalogues are constructed from the same parent simulation, the scatter between statistics estimated from them might underestimate the true sampling variance.

All observation points were chosen with the following criteria:

- (i) observation point is  $> 15 h^{-1}$  Mpc from the edge of the simulation box.
- (ii) a massive ( $\sim 5 \times 10^{14} h^{-1} M_\odot$ ) Virgo-type halo is located within a distance of  $\sim 20 h^{-1}$  Mpc.

We did not restrict the local  $< 10 h^{-1}$  Mpc environment of the observation points by any criteria. Although it is not clear if choosing an observation point simply by the two former criteria resolves the environment issue, we believe this to be strict enough for the statistical study of the virial ratio of groups. These criteria are justified for the statistical study, as we did not perceive a significant difference between the observation points in the low-resolution simulation. Small differences between observation points were observed when the high-resolution simulation was studied, as it only includes two Virgo-type haloes. When the low-resolution simulation was studied, the location of a massive (Virgo-type) halo did not have any significant effect to our results.

The simulation data do not directly give the luminosity or the absolute magnitude of the dark matter haloes, which are needed when we are mimicking observational conditions. We use haloes’ virial mass  $M_{\text{vir}}$  to obtain its luminosity. To obtain the luminosity of an object in the blue band, we use the relation proposed by Vale & Ostriker (2004):

$$L(M_{\text{vir}}) = 5.7 \times 10^9 h^{-2} L_\odot \frac{M_{11}^p}{[q + M_{11}^{s(p-r)}]^{1/s}}, \quad (16)$$

where  $M_{11}$  is defined:

$$M_{11} = \frac{M_{\text{vir}}}{10^{11} h^{-1} M_\odot}. \quad (17)$$

For the free parameters of the mass-luminosity function, values of  $p = 4.0$ ,  $q = 0.57$ ,  $r = 0.28$  and  $s = 0.23$  were adopted (Oguri 2006). It has been shown by Cooray & Milosavljević (2005) that the relation between the mass of a dark matter halo and its luminosity is not as straightforward as presented above. For our purposes, as the luminosity of a dark matter halo is used only to determine whether a halo is visible from the observation point, the above relation should be satisfactory. For this work, we do not adopt more complex methods such as actual distributions for the mass–luminosity relation.

After the luminosity  $L$  of the halo is known, we obtain the apparent magnitude of the halo in the blue band from the equation:

$$m_B = M_{\odot_B} - 2.5 \log_{10} \left( \frac{L}{L_\odot} \right) + 5 \log_{10} \left( \frac{d}{1 \text{ Mpc}} \right) + 25, \quad (18)$$

where  $d$  is the distance from the observation point and the magnitude of the sun in blue band  $M_{\odot_B} = 5.47$  (Cox 2000). As seen from equation (18), we do not include dust extinction in our study, as its effect in a statistical study like ours would be negligible.

The method described above allows us to use the apparent magnitude limit  $m_{\text{lim}} = 13.2$  as adopted in HG82. Group catalogues of this study are also generated with different magnitude limits in order to understand the effects of the magnitude limit in magnitude-limited samples. Unless explicitly noted, all haloes and groups referred to are from the simulations; real groups of galaxies from HG82 and UZC-SSRS2 (Ramella et al. 2002) are denoted as such.

### 5.2 Comparison parameters

We begin by calculating the velocity dispersion  $\sigma_v$  of a group. In general, the velocity dispersion of a group is defined as

$$\sigma_v = \sqrt{\frac{1}{N_H - 1} \sum_{i=1}^{N_H} (v_i - \langle v_R \rangle)^2}, \quad (19)$$

where  $N_H$  is the number of haloes (or galaxies) in a group,  $v_i$  is the radial velocity of the  $i$ th halo (or galaxy) and  $\langle v_R \rangle$  is the mean group radial velocity.

The second comparison parameter is the mean pairwise separation  $R_p$  which is a measure of the size of a group. It can be defined as

$$R_p = \frac{8 \langle v_R \rangle}{\pi H_0} \sin \left[ \frac{1}{N_H(N_H - 1)} \sum_{j < i}^{N_H} \sum_{i=1}^{N_H} \theta_{ij} \right], \quad (20)$$

where  $\langle v_R \rangle$  is the mean group radial velocity,  $H_0$  is the Hubble constant and  $\theta_{ij}$  is the angular separation of the  $i$ th and  $j$ th group members. Other two comparison parameters are the total group mass and the virial crossing time (in units of the Hubble time  $H_0^{-1}$ ) which can be defined as

$$t_c = \frac{3 R_H}{5^{3/2} \sigma_v}, \quad (21)$$

where  $\sigma_v$  is the velocity dispersion and  $R_H$  is the mean harmonic radius:

$$R_H = \frac{\pi \langle v_R \rangle}{H_0} \sin \left\{ \frac{1}{2} \left[ \frac{N_H(N_H - 1)}{2} \left( \sum_{i=1}^{N_H} \sum_{j>i}^{N_H} \theta_{ij} \right)^{-1} \right] \right\}, \quad (22)$$

where all the variables are defined as above.

In observations, the group masses can be estimated in various methods. In the HG82 and the UZC-SSRS2 catalogues, the total mass of a group is estimated with a simple relation:

$$M_{\text{obs}} = 6.96 \times 10^8 \sigma_v^2 R_H M_{\odot}, \quad (23)$$

where  $\sigma_v$  is the velocity dispersion and  $R_H$  is the mean harmonic radius of the group as defined above. We use this simple relation to determine the ‘observable’ mass of a group when we are comparing the masses of the simulated groups to the real observed groups such as HG82 and UZC-SSRS2. However, when the total mass of a group is used to scale the properties of groups (in Section 6), we calculate the total mass of a group of dark matter haloes as a sum of the member halo masses, namely the ‘true’ mass of the group. In case of the subhaloes, the diffuse dark matter is included in the main halo’s mass. In general, we do not include the diffuse dark matter within a given distance from the group centre, as it would be troublesome to choose an appropriate distance. We do not consider this error to be meaningful, as the diffuse dark matter does not substantially give rise to the mean density of a simulation.

### 5.3 Comparison with observations

Comparison between simulations and observations is done using a Kolmogorov–Smirnov (K–S) test. The null hypothesis  $H_{\text{null}}$  of the K–S test is that the two distributions are alike and are drawn from the same population distribution function. Results of the K–S tests are presented as significance levels (value of the  $Q$  function) for the null hypothesis. Correlation between two variables is proved or disproved with the use of the linear correlation coefficient  $r$ . In general, the significance level of 0.001 is adopted when the correlation between two variables is determined. For correlations, we also present a probability  $P(r)$  of observing a value of the correlation coefficient greater than  $r$  for a sample of  $N$  observations with  $N - 2$  degrees of freedom.

We begin the comparison of our simulations to observations by using the parameters presented in the previous subsection. A direct comparison between HG82 and simulations is possible as the magnitude limit (13.2) and the depth of the catalogues ( $cz < 4000 \text{ km s}^{-1}$ ) are comparable. Comparisons with the more recent group catalogue UZC-SSRS2 are also done. The UZC-SSRS2 catalogue has the magnitude limit of 15.5 and only galaxies with  $cz < 15000 \text{ km s}^{-1}$  has been considered. These differences make the direct comparison of the UZC-SSRS2 with the simulations less conclusive. We also compare our 10 observation points with each other but do not find significant difference between them. This justifies our method of choosing the observational points as stated before.

In Figs 1–5, the abundance of groups is scaled to the volume of a sample as the distributions depend strongly on selection and volume effects. However, as there is no ‘total’ volume of a galaxy sample in magnitude-limited group catalogues, we weight each group according to its distance (Moore et al. 1993; Diaferio et al. 1999). As we only consider groups with three or more members, we can identify a group only when its third-brightest galaxy has an absolute

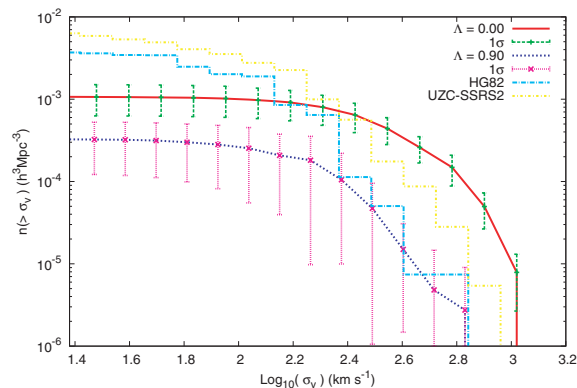


**Figure 5.** The cumulative distribution of velocity dispersion  $\sigma_v$  for galaxy groups from two different simulations with two different values of the cosmological constant  $\Omega_\Lambda$  when the apparent magnitude limit of 13.2 has been adopted. The simulation data are averaged over the ensemble of 10 mock catalogues. For comparison also the observational data from the HG82 and the UZC-SSRS2 catalogue have been plotted. The standard  $\Omega_\Lambda = 0.73$  simulations are shown in Fig. 1.

magnitude

$$M_i \leq m_{\text{lim}} - 25 - 5 \log \left( \frac{\langle cz \rangle}{H_0} \right), \quad (24)$$

where  $\langle cz \rangle$  is the mean velocity of the group.  $M_i$  determines the radius  $cz_i$  of a sphere within which we could have identified this group.

We calculate the comoving volume sampled by a group with the following equation:

$$\Psi_i = \frac{\omega}{3} \left( \frac{cz_i}{H_0} \right)^3 \left[ 1 - \frac{3z_i}{2} \left( 1 + \frac{\Omega}{2} \right) \right], \quad (25)$$

where  $\omega$  is the solid angle of the catalogue,  $z_i$  is the redshift of the group,  $c$  is the speed of light and  $\Omega$  is the cosmological density parameter, taken as 1.0. Each group of galaxies (or dark matter haloes) contributes with a weight of  $\Psi_i^{-1}$  to the total abundance of groups. We include all galaxies with  $cz > 500 \text{ km s}^{-1}$ . This lower cut-off avoids including faint objects that are close to the observation point as these groups could contain galaxies fainter than real magnitude-limited surveys. Therefore, we consider only groups with  $\langle cz \rangle$  larger than  $500 \text{ km s}^{-1}$  in mock, HG82 and UZC-SSRS2 catalogues.

Figs 1–4 show that the  $\Lambda$ CDM simulations are, in general, in a moderate agreement with observations when the resolution effects of the  $N$ -body simulations are taken into account. Our  $\Lambda$ CDM simulations are within  $2\sigma$  from the UZC-SSRS2 catalogue and within  $3\sigma$  from the HG82 catalogue. Figs 1–4 are all from the  $\Omega_\Lambda = 0.73$  simulations when the apparent magnitude limit has been set to 13.2, comparable to HG82. The error bars in Figs 1–4 are the standard deviation between 10 observation points. Unless explicitly noted, the simulations referred to are  $\Omega_\Lambda = 0.73$  simulations, other models are denoted as such.

#### 5.3.1 Velocity dispersion

Fig. 1 shows that the cosmological  $\Omega_\Lambda = 0.73$  model can produce velocity dispersions similar to observations (see also Klypin et al. 2003; Macció et al. 2005; Peirani & de Freitas Pacheco 2006). Fig. 1 agrees with results by Casagrande & Diaferio (2006) (their fig. 14) even though Casagrande & Diaferio (2006) considered only groups



with  $>5$  members. Our low-resolution simulation produces roughly the right number density of groups when the high ( $>100 \text{ km s}^{-1}$ ) velocity dispersions are considered and the comparison is carried out against more recent observations (UZC-SSRS2). However, due to the limited mass resolution, the low-resolution simulation lacks a significant number of groups when the abundance of groups with velocity dispersions  $<100 \text{ km s}^{-1}$  is studied. Because of this discrepancy, the applied K–S test fails:  $Q \sim 10^{-6}$  (against the HG82) and  $Q \sim 10^{-6}$  (against the UZC-SSRS2). Even though the K–S test fails, the low-resolution simulation is within  $3\sigma$  from the HG82. When the high-resolution simulation is considered, we get roughly the same number density of groups as in observations. However, the high-resolution simulation lacks groups with velocity dispersions  $>500 \text{ km s}^{-1}$ . This can be explained by the small volume of the high-resolution simulation. Even with this discrepancy, the applied K–S tests are approved with the significance levels of 0.02. When observations (HG82 and UZC-SSRS2) are compared against each other, the applied K–S test is approved at level of 0.34. For detailed significance levels of the K–S tests, see Table 3.

### 5.3.2 Mass

Fig. 2 shows that the cosmological  $\Lambda$ CDM model can produce ‘observable’ masses (equation 23) similar to observations when the resolution effects of the simulations are considered. The low-resolution simulation can produce the same number density of groups as in the UZC-SSRS2 catalogue when massive [ $\log(\text{Group Mass } M_{\odot}^{-1}) > 13.5$ ] groups are considered. Both the UZC-SSRS2 catalogue and the low-resolution mock catalogue has an excess of massive groups if comparison is carried out against the HG82 catalogue. When less massive groups [ $\log(\text{Group Mass } M_{\odot}^{-1}) < 13.0$ ] are studied, the low-resolution simulation has a number density of groups which is over  $3\sigma$  lower than in the UZC-SSRS2 catalogue. The resolution effect is clearly visible in Fig. 2 when the high-resolution simulation is studied, as it can produce about the right number density of groups when less massive [ $\log(\text{Group Mass } M_{\odot}^{-1}) < 13.0$ ] groups are considered. The high-resolution simulation is less than  $1\sigma$  away from the HG82 and within  $2\sigma$  from the UZC-SSRS2 even when groups with  $\log(\text{Group Mass } M_{\odot}^{-1}) < 11.0$  are considered. The applied K–S test is approved ( $Q \sim 0.58$ ) only when the high-resolution simulation is compared to the HG82 catalogue. In all other cases, the K–S test fails. For numerical details of the K–S test, see Table 3.

As the ‘observable’ mass of a group depends strongly on the groups’ velocity dispersion (see equation 23), we made another comparison between group abundances by mass. If we use the ‘true’ mass of a group instead of an ‘observable’ mass, other differences arise. There is no substantial difference between the plots of ‘observable’ and ‘true’ mass when comparing the abundances of lighter [ $\log(\text{Group Mass } M_{\odot}^{-1}) < 14.0$ ] groups. However, our simulations do not produce a single group with a ‘true’ mass  $>5 \times 10^{14} h^{-1} M_{\odot}$ . The low- and the high-resolution  $\Omega_{\Lambda} = 0.73$  simulations show the same cut-off, thus the lack of massive groups is not a resolution effect. However, the small volume of our simulation boxes explains the lack of massive groups in simulations and the existence of groups with large ‘observed’ mass is due to projection effects, which are not reliably taken into account in equation (23).

### 5.3.3 Size

The cosmological  $\Omega_{\Lambda} = 0.73$  model can produce groups of haloes which are similar in size to observed groups. Note, however, that

we do not compare our simulations to the UZC-SSRS2 catalogue, as it does not contain the information about the pairwise separation of groups. Our high-resolution simulation produces about the right number density of groups when small [ $\log(R_p) < -0.4$ ] groups are considered and the error is well within  $1\sigma$ . The high-resolution simulation seems to produce an excess of groups, when intermediate size ( $\log(R_p) \in [-0.3, 0.4]$ ) groups are considered. However, as the only comparison observation is the HG82 catalogue this excess might not be as large as in Fig. 3, as other comparisons (Figs 1 and 2) show that the HG82 and the UZC-SSRS2 catalogues differ quite significantly from each other.

When the low-resolution simulation is studied, we observe this same excess when larger [ $\log(R_p) > 0.1$ ] groups are considered. Because of these discrepancies, the applied K–S test fails in both cases, with  $Q \sim 10^{-3}$  and  $Q \sim 10^{-5}$  for the high- and the low-resolution simulations, respectively. Even though the K–S test fails, the simulated mock catalogues of group abundances by mean pairwise separation are mostly within  $2\sigma$ .

### 5.3.4 Crossing time

Fig. 4 shows that the cosmological  $\Omega_{\Lambda} = 0.73$  model can produce groups with crossing times similar to the HG82 observations. The low-resolution simulation produces the number density of groups with small crossing times, which is a lot lower than observed. However, this discrepancy is due to limited resolution, as the high-resolution simulation produces a lot more groups with small crossing times. The high-resolution simulation produces roughly the right number density of groups when the crossing time of the group is studied. Some differences are observed when larger [ $\log(t_c) > -0.6$ ] crossing times are studied. Both simulations produce a higher number density than observed. For low-resolution simulation, this excess is not large as the number density is within  $2\sigma$ . Because of the discrepancies visible in Fig. 4, the applied K–S test fails in both cases. For numerical details, see Table 3. When more recent values of the Schechter luminosity function are adopted, somewhat lower crossing times are observed in general. However, more recent values of the Schechter luminosity function do not give a better agreement, and the K–S test fails. The significance levels of the K–S tests are  $\sim 10^{-4}$  and  $\sim 10^{-5}$ , respectively.

Our simulations with the FOF algorithm do not (with a few exceptions) contain groups with crossing time larger than one Hubble time. For the high-resolution simulation, the median value of the crossing time is  $0.14H_0^{-1}$ . The median value of the crossing time for the HG82 catalogue and for the low-resolution simulation is  $0.19H_0^{-1}$ . Small crossing times suggest that groups of galaxies have had time to virialize and these groups should be gravitationally bound (see e.g. Gott & Turner 1977; Tucker et al. 2000; Aceves & Velázquez 2002; Plionis, Basilakos & Ragone-Figueroa 2006). We studied the correlation between crossing time and virial ratio, and did not find any significant relation between these two variables. The linear correlation coefficient of  $-0.01$  suggests that there is no correlation between crossing time and virial ratio, in the low-resolution simulation when the apparent magnitude limit of 13.2 is adopted. This correlation is not significant at level of 0.05 and  $P(r) \sim 0.29$ . There is no significant correlation between these two variables when different values of  $\Omega_{\Lambda}$ , resolutions or the apparent magnitude limits are adopted (see Table 2). The lack of correlation between virial ratio and crossing time (see similar results in Diaferio et al. 1993) calls into question the crossing time as an estimator of gravitationally bound systems which is widely accepted in observations.

**Table 2.** The correlation between crossing time and virial ratio when different values of  $\Omega_\Lambda$  and the apparent magnitude limits are adopted.

$\Omega_\Lambda$	$m_{\text{lim}}$	$r$	$\alpha$	$P(r)$
0.00	13.2	-0.009	>0.05	0.33
0.00	20.0	0.005	>0.05	0.36
0.73 <sup>H</sup>	13.2	-0.016	>0.05	0.26
0.73 <sup>L</sup>	13.2	-0.016	>0.05	0.29
0.73 <sup>L</sup>	20.0	-0.016	>0.05	0.09
0.90	13.2	-0.012	>0.05	0.42
0.90	20.0	-0.022	>0.05	0.09

Note:  $\Omega_\Lambda$  specifies the value of the cosmological constant (<sup>H</sup> = high-resolution simulation and <sup>L</sup> = low-resolution simulation),  $m_{\text{lim}}$  is the apparent magnitude limit of the search,  $r$  is the value of the linear correlation coefficient,  $\alpha$  is the significance level and  $P(r)$  is the probability of observing a value of the correlation coefficient greater than  $r$ .

### 5.3.5 Richness

The  $\Omega_\Lambda = 0.73$  model can produce groups comparable to observations when the number of members in a group is studied. The abundance of ‘rich’ groups is roughly the same in the low-resolution simulation as in the observations. However, the low-resolution simulation cannot produce as many ‘poor’ groups as is observed. The lack of ‘poor’ (<4) and the excess of ‘intermediate’ ( $\in [6, 40]$ ) groups are the reason why the K–S test fails ( $Q \sim 10^{-5}$ ). The agreement is even worse ( $Q \sim 10^{-7}$ ) when more recent values of Schechter luminosity function are adopted. These values ( $\alpha = -1.15$ ,  $M^* = -19.84$ , and  $\Phi^* = 0.0172$ ) produce a large number of ‘poor’ groups and a lack of ‘rich’ groups. The difference between the low-resolution simulation and observations is due to the limited resolution in the simulations. When the high-resolution simulation is used, the agreement to observations, especially to UZC-SSRS2, is better ( $Q \sim 10^{-3}$ ).

### 5.3.6 Influence of dark energy

There are big differences between different cosmological models when dynamical properties of groups of dark matter haloes are studied. Fig. 5 shows the impact of dark energy on the formation of galaxy groups. It is clear that the  $\Omega_\Lambda = 0.0$  simulation over produces groups with high-velocity dispersions. The excess is over  $3\sigma$  if the comparison is carried out to the HG82 catalogue. A smaller discrepancy is observed when the comparison is carried out to the UZC-SSRS2 catalogue. The small number density of small velocity dispersion groups can be explained by the resolution effect which is also visible in Fig. 1. Because of these discrepancies the K–S tests fails. When the  $\Omega_\Lambda = 0.90$  simulation is studied, a qualitatively better agreement is observed, especially when the comparison is carried out to the HG82 catalogue. The great difference in the number density of small velocity dispersion groups can be explained by the resolution effect and the fact that the  $\Omega_\Lambda = 0.90$  simulation has relatively small number of groups. Because of the great discrepancy in the number density of small velocity dispersion groups, the applied K–S test fails in both cases.

The  $\Omega_\Lambda = 0.0$  cosmology produces more massive groups with greater velocity dispersion than the  $\Lambda$ CDM cosmology. Larger number of massive groups can partially be explained by the somewhat lower mass resolution in the  $\Omega_\Lambda = 0.0$  simulation. However, the excess of massive groups is most likely due to equation (23), which we use to obtain the ‘observable’ mass of a group, which depends strongly on the velocity dispersion of the group. For numerical details of K–S tests, see Table 3.

**Table 3.** Comparison of HG82, UZC-SSRS2 and simulations when the apparent magnitude limit of 13.2 is adopted.

$\Omega_\Lambda$		HG82	UZC-SSRS2	HG82 versus UZC-SSRS2
0.00	$\sigma_v$	$10^{-5}$	$10^{-6}$	0.34
0.73 <sup>H</sup>	$\sigma_v$	0.02	0.02	0.34
0.73 <sup>L</sup>	$\sigma_v$	$10^{-6}$	$10^{-6}$	0.34
0.90	$\sigma_v$	$10^{-6}$	$10^{-7}$	0.01
0.00	$M_G$	$10^{-5}$	$10^{-6}$	$10^{-3}$
0.73 <sup>H</sup>	$M_G$	0.58	$10^{-5}$	$10^{-3}$
0.73 <sup>L</sup>	$M_G$	$10^{-6}$	$10^{-6}$	$10^{-3}$
0.90	$M_G$	$10^{-6}$	$10^{-7}$	$10^{-3}$
0.73 <sup>H</sup>	$R_p$	$10^{-3}$	–	–
0.73 <sup>L</sup>	$R_p$	$10^{-5}$	–	–
0.73 <sup>H</sup>	$t_c$	$10^{-4}$	–	–
0.73 <sup>L</sup>	$t_c$	$10^{-5}$	–	–

Note: Significance levels of the K–S test for the null hypothesis that observations and the simulations (<sup>H</sup> = high resolution and <sup>L</sup> = low resolution) are alike and are drawn from the same parent population (HG82 and UZC-SSRS2 columns). Significance levels of the K–S test for the null hypothesis that the HG82 and the UZC-SSRS2 group catalogue are alike and are drawn from the same parent population (HG82 versus UZC-SSRS2 column).

### 5.3.7 Median values and other properties

The median values of the group properties are presented in Table 4. In general, our simulations seem to produce groups which median value of the velocity dispersion and the group mass is greater than in observations. In simulations, groups have also a greater median value for the mean pairwise separation than in the HG82 sample. The  $\Omega_\Lambda = 0.73$  simulations have the median value of velocity dispersions which are close to observations, even though they are somewhat higher. In general, median values of the group properties are in a moderate agreement with the results of similar studies (e.g. Diaferio et al. 1999; Casagrande & Diaferio 2006). Casagrande & Diaferio (2006) found larger values for the median velocity dispersions and group masses, but they considered only groups with >5 members, which most likely makes the median values of groups somewhat higher.

The fractions of isolated galaxies, binary galaxies and groups of galaxies were also studied. If we compare our results with HG82, a significant difference in the fraction of isolated galaxies is noted. Comparison to the Lyon-Meudon Extragalactic Database (LEDA) (Giudice 1999) catalogue shows a better fit (for more details, see Table 5). Tucker et al. (2000) listed a large fraction of galaxies in groups from different group catalogues. These results and comparisons are not shown in this paper due to the different magnitude limits and grouping algorithms adopted in those observations. We may state that, in general, simulations show similar results to observations (excluding HG82), with regard to the fractions of groups, binaries and isolated galaxies.

We also made an attempt to study discordant redshifts in compact groups observed, for example, by Sulentic (1984) and Girardi et al. (1992). This effect has been studied by several authors (see e.g. Byrd & Valtonen 1985; Valtonen & Byrd 1986; Iovino & Hickson 1997) who have come up with different explanations. According to these authors, apparent discordant redshifts arise when groups are not virialized and their central galaxies are incorrectly identified. Our findings are not conclusive as we did not have any exact method to identify which dark matter haloes might represent observable spiral galaxies. We did not observe any significant asymmetry in the radial velocities of the groups and neither this asymmetry was seen in the



**Table 4.** Weighted quartiles of the group properties.

	$\Omega_\Lambda = 0.00$	$\Omega_\Lambda = 0.73^{\text{H}}$	$\Omega_\Lambda = 0.73^{\text{L}}$	$\Omega_\Lambda = 0.90$	HG82	UZC-SSRS2
$\sigma_v$	178/307/403	135/180/295	103/160/298	124/209/271	60/135/155	60/130/178
$\log M_G$	13.6/14.0/14.4	12.7/13.2/13.5	12.8/13.6/14.0	12.7/13.1/13.5	12.0/12.4/13.2	12.1/12.8/13.3
$R_p$	0.85/1.38/1.57	0.81/1.21/1.47	0.80/0.99/1.24	0.72/1.01/1.20	0.44/0.54/1.00	–
$t_c$	0.09/0.14/0.25	0.07/0.14/0.19	0.10/0.19/0.27	0.09/0.17/0.23	0.10/0.19/0.27	–

Note: Quantities  $\sigma_v$ ,  $\log M_G$ ,  $R_p$  and  $t_c$  are in units of  $\text{km s}^{-1}$ ,  $h^{-1} M_\odot$ ,  $h^{-1} \text{Mpc}$  and Hubbles, respectively.

**Table 5.** Fractions of isolated galaxies, binary galaxies and groups.

Source	$m_{\text{lim}}$	Groups (per cent)	Binaries (per cent)	Isolated (per cent)
Simu	13.2	$38.1 \pm 0.5$	$19.7 \pm 0.1$	$42.2 \pm 0.5$
Simu	20.0	$41.2 \pm 0.2$	$17.6 \pm 0.1$	$41.2 \pm 0.2$
HG82	13.2	60.0	14.0	26.0
LEDA	14.0	$33.3 \pm 0.5$	$17.1 \pm 0.3$	$49.6 \pm 0.4$

Note: Source refers to the sample (Simu = the low-resolution  $\Omega_\Lambda = 0.73$  simulation),  $m_{\text{lim}}$  is the apparent magnitude limit [in  $m_{B(0)}$  except for LEDA in  $B_T^0$ ], Groups (per cent) is the fraction of galaxies in the groups, Binaries (per cent) is the fraction of galaxies forming double systems and Isolated (per cent) is the fraction of galaxies which are not classified into any group or double system. Poisson error limits have been calculated for the samples.

groups, which were misidentified (so that the brightest member is not the dominant member). No significant difference for the radial velocity asymmetry was discovered between bound and unbound groups.

## 6 GRAVITATIONALLY BOUND GROUPS

Gravitationally bound groups are determined by using the criterion (virial ratio, equation 15) presented in Section 3. This method of computing the gravitational potential well of a group does assume that the group is isolated. This is not strictly true as each group is embedded in the large-scale matter distribution, which might have an effect to the threshold 1.0 of the virial rati $\mathit{on} T/U$ . However, we believe this effect to be negligible in a statistical study like ours.

Our study shows that  $\sim 20$  per cent of groups generated by the FOF algorithm are not gravitationally bound when the  $\Omega_\Lambda = 0.73$  model is adopted. This result is in agreement with Diaferio et al. (1994), who derived a similar result for the compact groups of galaxies. If we vary the apparent magnitude limit of the search from the original 13.2–20.0, even more groups ( $\sim 37$  per cent) are unbound. This is not a negligible fraction considering that one widely accepted and applied method of calculating a group mass, from observations, is based on the assumption that groups found by the FOF algorithm are, in general, gravitationally bound systems.

If we vary the value of the cosmological constant from the original 0.73–0.90, a slightly larger fraction of groups seems to be unbound when the apparent magnitude limit of 13.2 is adopted. This result is intuitively reasonable. If the negative vacuum pressure of space is larger, gravitational force becomes ‘weaker’ and a smaller number of dark matter haloes are formed and fewer groups are gravitationally bound objects. How does the fraction of gravitationally unbound groups change, when the negative vacuum pressure of space is lowered? If the value of the cosmological constant is put to 0.0, about the same fraction of groups (with  $m_{\text{lim}} = 13.2$ ) are spurious as in the  $\Omega_\Lambda = 0.90$  cosmology. When the apparent magnitude limit is

**Table 6.** Fractions of gravitationally bound groups of dark matter haloes when different cosmological models and apparent magnitude limits have been adopted.

$\Omega_\Lambda$	$m_{\text{lim}}$	$N_{\text{groups}}$	$f_{\text{bound}}$ (per cent)	$N_{\text{isolated}}$ (per cent)
0.00	13.2	2675	79.2	20.9
0.00	20.0	6213	64.5	41.8
0.73 <sup>H</sup>	13.2	1570	70.1	32.8
0.73 <sup>L</sup>	13.2	1168	81.1	42.2
0.73 <sup>L</sup>	20.0	6807	62.7	41.2
0.90	13.2	238	77.3	53.1
0.90	20.0	3678	62.0	36.5

Note:  $\Omega_\Lambda$  specifies the value of the cosmological constant (<sup>H</sup> = high-resolution stimulation and <sup>L</sup> = low-resolution simulation),  $m_{\text{lim}}$  is the apparent magnitude limit of the search,  $N_{\text{groups}}$  is the number of groups found from 10 observation points,  $f_{\text{bound}}$  is the fraction of gravitationally bound groups and  $N_{\text{isolated}}$  is the percentage of the isolated haloes which do not belong to any group or binary system.

changed to 20.0,  $\sim 37$  per cent of the groups are spurious (for details, see Table 6).

In the low-resolution  $\Omega_\Lambda = 0.73$  simulation, the fraction of gravitationally bound groups rises from 81.1 to 81.7 per cent, when more recent values of the Schechter luminosity function are adopted. Meanwhile the total number of groups decreases  $\sim 10.0$  per cent. The fraction of gravitationally bound groups rises from 81.1 to 82.8 per cent, when the values of the free parameters of  $D_0 = 0.37 \text{ Mpc}$  and  $V_0 = 200 \text{ km s}^{-1}$  are adopted. This result agrees with Frederic (1995a,b) who obtained similar result while studying group accuracy as a function of  $D_0$  and  $V_0$ . Frederic (1995a,b) showed that smaller values of  $D_0$  and  $V_0$  produce groups with greater accuracy and these groups should be gravitationally bound.

Adopting the values of  $D_0 = 0.37 \text{ Mpc}$  and  $V_0 = 200 \text{ km s}^{-1}$  have a significant effect to the total number of groups found from the simulations. The low-resolution  $\Omega_\Lambda = 0.73$  simulation produces, in all, 1168 groups of dark matter haloes, when the original values ( $D_0 = 0.63 \text{ Mpc}$  and  $V_0 = 400 \text{ km s}^{-1}$ ) of the free parameters are adopted. When  $D_0 = 0.37 \text{ Mpc}$  and  $V_0 = 200 \text{ km s}^{-1}$  are adopted, the total number of groups found from the low-resolution simulation drops to 661 while the fraction of isolated haloes rises from  $\sim 42.2$  to  $\sim 64.9$  per cent. Also, the group abundances change significantly as the richest group found from the low-resolution simulation with  $D_0 = 0.37 \text{ Mpc}$  and  $V_0 = 200 \text{ km s}^{-1}$  has only 15 members. These results are due to the fact that the limiting density enhancement of the search is inversely proportional to  $D_0^3$ .

Our study shows that the  $\Omega_\Lambda = 0.00$  model produces about the same fraction of bound groups as the  $\Omega_\Lambda = 0.90$  model, when the apparent magnitude limit is 13.2. However, the  $\Omega_\Lambda = 0.73$  model produces more gravitationally bound systems than the two other models we study when the original apparent magnitude limit is adopted. If the apparent magnitude limit is changed to 20.0, the  $\Omega_\Lambda = 0.00$  model

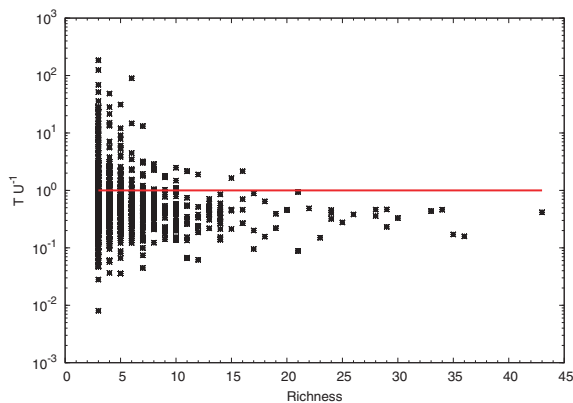


**Figure 6.** Virial ratio ( $TU^{-1}$ ) versus the number of members in a group (Richness). Groups with more than 10 members are more often bound than ‘poor’ groups with three to five members. The data are from the low-resolution  $\Omega_{\Lambda} = 0.73$  simulation when the apparent magnitude limit of 13.2 has been adopted.

**Table 7.** Fractions of gravitationally bound ‘poor’ and ‘rich’ groups of dark matter haloes generated from the low-resolution  $\Omega_{\Lambda} = 0.73$  simulation.

$m_{\text{lim}}$	$N_{\text{haloes}}$	$N_{\text{groups}}$	$f_{\text{bound}}$ (per cent)
13.2	3	448	77.0
13.2	$\in [3, 4]$	697	78.5
13.2	$>4$	471	84.9
20.0	3	2786	55.6
20.0	$\in [3, 4]$	4147	56.3
20.0	$>4$	2660	72.6

*Note:*  $m_{\text{lim}}$  is the apparent magnitude limit of a sample,  $N_{\text{haloes}}$  is the number of haloes in a group,  $N_{\text{groups}}$  is the number of groups found from 10 observation points with appropriate number of haloes and  $f_{\text{bound}}$  is the fraction of gravitationally bound groups.

produces a slightly larger fraction of gravitationally bound groups than the  $\Omega_{\Lambda} = 0.73$  or the 0.90 simulations (for details, see Table 6). The use of the apparent magnitude limit of 20.0 means simply that every single dark matter halo in a simulation box is visible at the observation point. This result is not without bias as the simulation box is of finite size and the edge effects might become significant, even using the periodic boundary conditions in the simulations.

The calculation that determines whether a group is bound is based on three parameters: the total mass of the group, the relative velocity of the group members and the physical size of the group. In the following, we will study how sensitive the result is on the values of these parameters. But first we will study the virial ratio as a function of the number of members in the group. Fig. 6 shows the virial ratio  $T/U$  as a function of the number of haloes in the group, namely richness. The data come from the low-resolution  $\Omega_{\Lambda} = 0.73$  simulation with  $m_{\text{lim}} = 13.2$ . There are, in all, 1168 groups of haloes seen from 10 different observation points. The fractions of bound ‘poor’ and ‘rich’ groups are shown in Table 7.

From Fig. 6, we see that groups with more than 10 members are most likely gravitationally bound and groups with three to five members are quite often unbound. Ramella et al. (1997) argues that among groups with three members, 50–75 per cent of groups are spurious. They also conclude that for groups with more than three members the fraction of spurious groups is less than 30 per cent and may be as small as 10 per cent. Our findings are similar, and

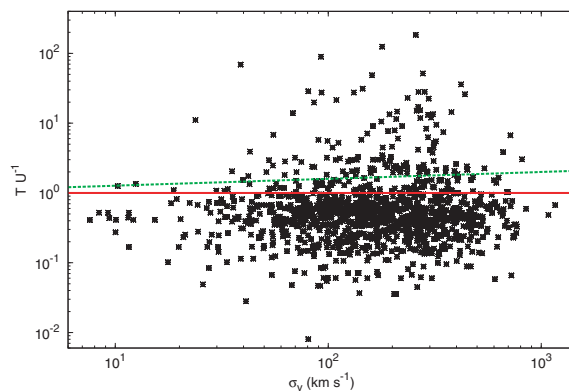


**Figure 7.** Virial ratio ( $TU^{-1}$ ) versus the velocity dispersion ( $\sigma_v$ ) of a group (in  $\text{km s}^{-1}$ ). The rms straight line has been fitted to the data. The data are from the low-resolution  $\Omega_{\Lambda} = 0.73$  simulation when the apparent magnitude limit of 13.2 has been adopted.

the fraction of bound groups with four or more members is about as high as Ramella et al. (1997) suggested. Ramella et al. (2002) find that for groups with five or more members at least 80 per cent of the groups are probably physical systems, but that 40–80 per cent of the groups with five or more members are bound groups. Our findings confirm the latter result. However, these results cannot be directly compared with ours, as slightly different values of the free parameters are adopted for the FOF algorithm. Even though the free parameters of the FOF seem to have only a small effect to the fraction of spurious groups in our study.

Our findings for the  $\Omega_{\Lambda} = 0.73$  cosmology are similar to Ramella et al. (1997) for ‘poor’ (three or four members) groups, as can be seen in Fig. 6 and Table 7. However, our findings do not confirm the claim by Ramella et al. (1997) that among groups with three members, 50–75 per cent of groups are spurious as we find only  $\sim 23$  per cent of groups with three members to be gravitationally unbound with  $m_{\text{lim}} = 13.2$ . For the apparent magnitude-limited sample ( $m_{\text{lim}} = 13.2$  comparable to HG82), we found  $\sim 21$  per cent of the groups with three or four haloes to be spurious. ‘Rich’ groups with five or more members are more often gravitationally bound than ‘poor’ groups, but the difference is relatively small at the apparent magnitude limit of 13.2 as for ‘rich’ groups, we found  $\sim 15$  per cent of the groups to be spurious. This is close to the upper limit proposed by Ramella et al. (1997, 2002). More details of our findings with different abundances and apparent magnitude limits are listed in Table 7.

In Fig. 7, the virial ratio is plotted as a function of the velocity dispersion  $\sigma_v$  of the group. The plot shows a weak correlation in the sense that groups with large velocity dispersion are more often gravitationally unbound than groups with small velocity dispersion. The linear correlation coefficient of 0.17 suggests that the correlation in Fig. 7 is weak. However, the correlation is significant at level of 0.001 and  $P(r) \sim 10^{-8}$ . The rms line plotted in Figs 7–11 is of the form  $\frac{T}{U} \propto \sigma_v^b$  or  $\frac{T}{U} \propto N(\text{haloes})^b$ . The value of the parameter  $b$  of the rms line in Fig. 7 is  $b = 0.10 \pm 0.04$ .

The weak trends are clearer if we scale the abscissa in both Figs 6 and 7 with the total mass of the group. Note that we use here the ‘true’ mass of a group rather than the ‘observable’ mass. Results are shown in Figs 8 and 9. More significant trends are now seen in both figures, even though the data are still scattered. The linear correlation coefficient of 0.32 suggests that a significant correlation exists between the number of haloes and the virial ratio when the first is scaled with the total mass of the group. The correlation in

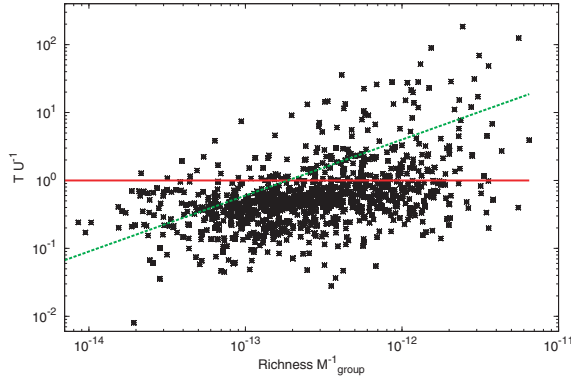


**Figure 8.** Virial ratio ( $TU^{-1}$ ) versus the number of members (Richness) in a group when the latter has been scaled with the total mass of the group ( $M_{\text{group}}^{-1}$  in  $h^{-1} M_{\odot}$ ). The rms straight line has been fitted to the data. The data are from the low-resolution  $\Omega_{\Lambda} = 0.73$  simulation when the apparent magnitude limit of 13.2 has been adopted.

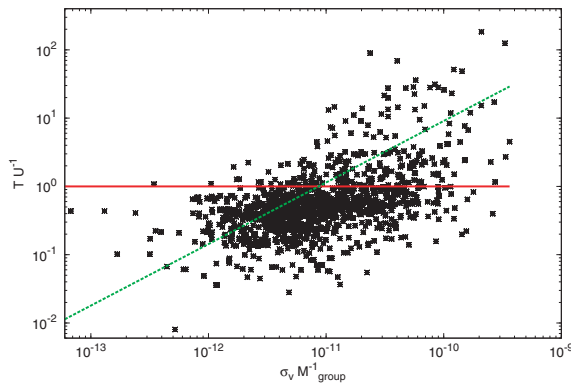
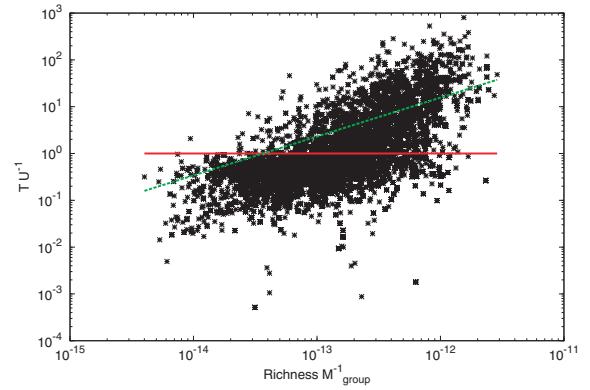


**Figure 9.** Virial ratio ( $TU^{-1}$ ) versus the velocity dispersion ( $\sigma_v$ ) of a group (in  $\text{km s}^{-1}$ ) when the latter has been scaled with the total mass of the group ( $M_{\text{group}}^{-1}$  in  $h^{-1} M_{\odot}$ ). The rms straight line has been fitted to the data. The data are from the low-resolution  $\Omega_{\Lambda} = 0.73$  simulation, when the apparent magnitude limit of 13.2 has been adopted.

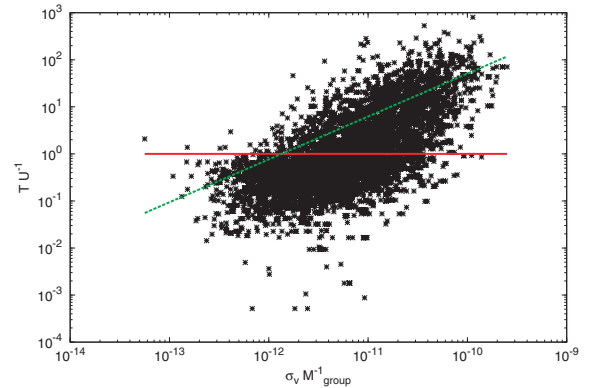
Fig. 8 is significant at level of 0.001 and  $P(r) < 10^{-25}$ . The slope of the rms line in Fig. 8 is  $b = 0.82 \pm 0.03$ .

Fig. 9 shows a strong trend, even though the data are still quite scattered. The linear correlation coefficient of 0.40 suggests that the correlation between the velocity dispersion of a group and the virial ratio of a group is quite strong. The correlation in Fig. 9 is significant at level of 0.001 and  $P(r) < 10^{-25}$ . The slope with standard errors of the rms line is now  $b = 0.90 \pm 0.03$ .

When the apparent magnitude limit is changed to 20.0, the trends of Figs 8 and 9 become stronger and the asymptotic standard errors for the rms lines become much smaller. The linear correlation coefficient of 0.62 shows that the correlation between the velocity dispersion of a group, and the virial ratio, is strong when the apparent magnitude limit of 20.0 is adopted. This correlation is significant at level of 0.001 and  $P(r) < 10^{-25}$ . What might be surprising is that changing the cosmological model, i.e. the value of the cosmological constant  $\Omega_{\Lambda}$ , does not have a substantial influence on Figs 9 and 10. The number of groups found from different simulations varies a lot as a function of  $\Omega_{\Lambda}$  but the fraction of gravitationally bound groups do not (see Table 6). For comparison with Figs 8 and 9, we show results from the  $\Omega_{\Lambda} = 0.0$  simulation in Figs 10 and 11. In these figures, the apparent magnitude limit of 20.0 has been adopted. Oth-



**Figure 10.** Virial ratio ( $TU^{-1}$ ) versus the number of members in a group (Richness) when the latter has been scaled with the total mass of a group ( $M_{\text{group}}^{-1}$  in  $h^{-1} M_{\odot}$ ), and  $\Omega_{\Lambda} = 0.0$  and  $m_{\text{lim}} = 20.0$  has been adopted. The rms straight line has been fitted to the data.



**Figure 11.** Virial ratio ( $TU^{-1}$ ) versus the velocity dispersion ( $\sigma_v$ ) of a group (in  $\text{km s}^{-1}$ ) when the latter has been scaled with the total mass of a group ( $M_{\text{group}}^{-1}$  in  $h^{-1} M_{\odot}$ ), and  $\Omega_{\Lambda} = 0.0$  and  $m_{\text{lim}} = 20.0$  has been adopted. Straight line is a rms fit to the data.

erwise, Figs 10 and 11 are comparable to Figs 8 and 9. The linear correlation coefficient in Figs 10 and 11 is: 0.32 and 0.65, respectively. Both of the correlations are significant at a level of 0.001 and  $P(r) < 10^{-25}$  for both samples. The asymptotic standard errors for the rms lines in Figs 10 and 11 are small:  $b = 0.83 \pm 0.02$  and  $0.91 \pm 0.01$ , respectively.

## 7 DISCUSSION

### 7.1 Probability functions of unbound groups

In this section, we briefly discuss a method, which gives a theoretical probability of a group being gravitationally unbound. The mass of the groups is assumed to be known. In observations, estimations of group masses are less than precise at best, therefore the applicability of this method to observational data is merely hypothetical. The observable quantities we study are the velocity dispersion divided by the group mass  $\sigma_v M_{\text{group}}^{-1}$  and the mean pairwise separation divided by the group mass  $R_p M_{\text{group}}^{-1}$ .

To calculate the probability functions for the groups, the first step is to choose an appropriate bin length (generally between 0.15 and 0.30) in the logarithm of the observable quantity. Then, one calculates the number of groups and the number of gravitationally

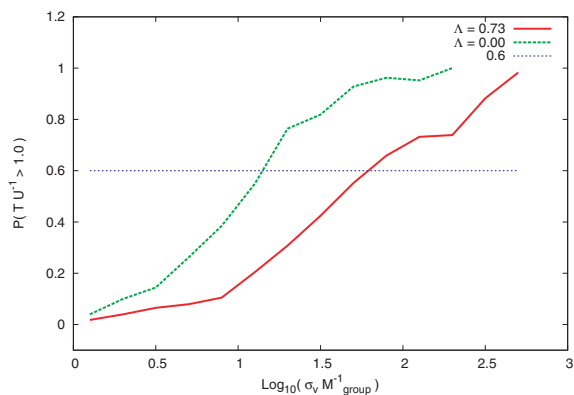


**Figure 12.** Unbound probability [ $P(TU^{-1} > 1.0)$ ] versus velocity dispersion [ $\sigma_v$ ] of a group when the  $\Omega_\Lambda = 0.73$  model, the apparent magnitude limit of 20.0, and a bin length of 0.2 are adopted.  $\sigma_v M_{\text{group}}^{-1}$  is in units of  $\text{km s}^{-1} (10^{12} h^{-1} M_\odot)^{-1}$ .

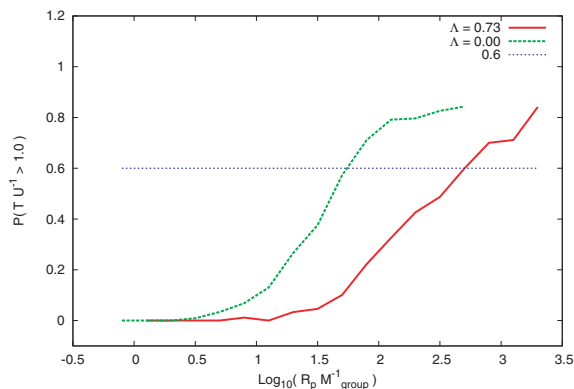


**Figure 13.** Unbound probability [ $P(TU^{-1} > 1.0)$ ] versus mean pairwise separation ( $R_p$ ) when the  $\Omega_\Lambda = 0.73$  model, the apparent magnitude limit of 20.0, and a bin length of 0.25 are adopted.  $R_p M_{\text{group}}^{-1}$  is in units of  $\text{Mpc} (10^{15} h^{-1} M_\odot)^{-1}$ .

bound groups in each bin and divides the number of unbound groups with the total number of groups in the bin. The logarithmic scale is chosen in order to lower the dispersion of the data and to assure a large enough number of groups in every bin.

The probability functions for the velocity dispersion  $\sigma_v$  and the mean pairwise separation  $R_p$ , normalized to the group mass, are shown in Figs 12 and 13. Fig. 12 shows that at values larger than 1.8 (the horizontal dotted line in Fig. 12) it is more probable that the groups are gravitationally unbound when the  $\Omega_\Lambda = 0.73$  model is adopted. The same result can also be inferred from Fig. 9, but with lower confidence.

The  $\Omega_\Lambda = 0.0$  simulation gives a probability function which is comparable to the probability function of the  $\Omega_\Lambda = 0.73$  model. It shows a similar linear growth as the probability function of the  $\Omega_\Lambda = 0.73$  model. However, the function is shifted along the horizontal axis. This shifting originates from the variation of the group masses and velocity dispersions (see Fig. 5). The change of the apparent magnitude limit does not have any significant effect on Fig. 12. When the apparent magnitude limit of 13.2 is adopted, a smaller number of haloes and groups are observed, which enlarges the variations between bins and gives a worse fit to a straight line.

The quantity  $\sigma_v M_{\text{group}}^{-1}$ , studied in Fig. 12, has a loose connection to the kinetic energy  $T$ . This connection explains the fact that the

lower normalized values of the quantity  $\sigma_v M_{\text{group}}^{-1}$  give gravitationally bound groups with a higher probability, and larger normalized values, loosely meaning the larger kinetic energies, give unbound groups with a higher probability.

The probability function of the mean pairwise separation (Fig. 13) shows a similar linear growth as the probability function of the velocity dispersion in Fig. 12. The variation from bin to bin is somewhat larger in the probability function of the mean pairwise separation due to the fact that the mean pairwise separation is not strictly the size of the group but it includes projection effects. The quantity  $R_p M_{\text{group}}^{-1}$ , studied in Fig. 13, is inversely proportional to the potential energy  $U$  if the mean pairwise separation is identified as the real size of a group. The difference between Figs 12 and 13 is understandable, as the velocity dispersion and the mean pairwise separation are not strictly connected to each other, although some loose relation exists as the equation of the mean pairwise separation includes the mean group radial velocity.

The  $\Omega_\Lambda = 0.90$  simulation shows similar probability functions as the  $\Omega_\Lambda = 0.0$  and 0.73 simulations. Figs 12 and 13 show that the  $\Omega_\Lambda$  does not have any significant effect for the fraction of gravitationally unbound groups. This result can also be inferred from Table 6. The small effect is hardly surprising as the theoretical studies (see e.g. Lahav et al. 1991) have predicted that the  $\Omega_\Lambda$  has little effect on the dynamics at the present epoch.

## 8 CONCLUSIONS

We have shown that the  $\Lambda$ CDM cosmology can produce groups of dark matter haloes comparable to observations of groups of galaxies when the FOF algorithm based on that of Huchra & Geller (1982) is adopted and the dynamical properties of groups are studied. Our groups from cosmological simulations are, in general, in a moderate agreement with observations, although a straight K–S test fails in most cases. Our  $\Omega_\Lambda = 0.73$  simulations are in satisfactory agreement with observations as the number densities of group properties are usually within  $2\sigma$  errors, or less, from the HG82 and the UZC–SSRS2 group abundances. The agreement between simulations and observations is good when the velocity dispersion and the ‘observable’ mass of groups are considered. In these cases, the applied K–S test is approved when the high-resolution  $\Omega_\Lambda = 0.73$  simulation is considered. The moderate agreement between simulations and observational data suggests that gravitational force alone is sufficient in order to explain the dynamical properties of groups of galaxies.

We have also shown that, in general, about 20 per cent of the groups of haloes generated with the algorithm presented in the HG82 are not gravitationally bound objects. The fraction of gravitationally bound groups of dark matter haloes varies with different values of the apparent magnitude limits. When the apparent magnitude limit is raised from the original 13.2–20.0, a larger number of spurious groups are found. The larger fraction of unbound groups with  $m_{\text{lim}} = 20.0$  could be explained by the fact that more interlopers are included into groups, when the apparent magnitude limit is increased. However, this analysis is beyond the scope of this study.

In general, a larger number of ‘rich’ groups are found when the apparent magnitude limit is lowered. This originates from the fact that more light haloes at close proximity to more massive haloes become visible and those light haloes are included into the groups. When the magnitude limit is raised from the original value of 13.2–12.0, a slightly larger fraction of the groups are found to be gravitationally bound. In general, fewer groups (in absolutely number) are found and these groups are ‘poorer’.

Small differences are found when the fractions of gravitationally bound ‘poor’ and ‘rich’ groups are studied. ‘Rich’ groups with more than four members are more often gravitationally bound than ‘poorer’ groups. This result agrees with previous ones (e.g. Ramella et al. 2002). Our results do not confirm the claim by Ramella et al. (1997) who argued that 50–75 per cent of groups with three members are spurious. Our results show that  $\sim 77$  per cent of groups containing only three members are gravitationally bound when the apparent magnitude limit of 13.2 is adopted.

When the value of the cosmological constant  $\Omega_\Lambda$  is varied, the fractions of unbound groups change only slightly. This is somewhat surprising as it would be intuitively expected that a larger value of the dark energy would lead to a greater number of groups that are not gravitationally bound. Some variation is observed when the fraction of gravitationally bound groups is studied as a function of the cosmological constant, but, in general, a significant number of groups remains unbound in all cases of  $\Omega_\Lambda$ .

When the values of the free parameters of the FOF algorithm are varied, the fraction of gravitationally bound groups can be raised from  $\sim 81$  to  $\sim 83$  per cent. A greater difference is observed when the fraction of isolated haloes is studied. Varying the values of  $D_0$  and  $V_0$  makes a great difference, raising the fraction of isolated haloes from  $\sim 42$  to  $\sim 65$  per cent. In general, we do not find any significant difference in the fractions of gravitationally bound groups when different values of  $D_0$  and  $V_0$  or parameters of the Schechter luminosity function are adopted.

In observations, the crossing time of a group is often taken as an indicator of the virialization. We do not find any correlation between the virial ratio and the crossing time of a group. This result does not depend on the chosen value of the apparent magnitude limit of the search, or the cosmological model adopted. The lack of the correlation between these two variables calls into question the crossing time as an estimator of the virialization.

## ACKNOWLEDGMENTS

This work is part of the master’s thesis of SMN at the University of Turku. SMN acknowledges the funding by the Finland’s Academy of Sciences and Letters. SMN would like to thank Dr. Alexander Knebe for his cosmological  $N$ -body simulation code AMIGA, professor Gene Byrd for helpful suggestions and the referee, Antonaldo Diaferio, for a number of invaluable corrections and suggestions. The cosmological simulations were run at the CSC - Finnish IT centre for science.

## REFERENCES

Aceves H., Velázquez H., 2002, *Rev. Mex. Astron. Astrofis.*, 38, 199  
 Berlind A. A. et al., 2006, *ApJS*, 167, 1  
 Byrd G. G., Valtonen M. J., 1985, *ApJ*, 289, 535

Carlberg R. G., Yee H. K. C., Morris S. L., Lin H., Hall P. B., Patton D. R., Sawicki M., Shepherd C. W., 2001, *ApJ*, 552, 427  
 Casagrande L., Diaferio A., 2006, *MNRAS*, 373, 179  
 Chernin A. D., Mikkola S., 1991, *MNRAS*, 253, 153  
 Cooray A., Milosavljević M., 2005, *ApJ*, 627, L89  
 Cox A. N., 2000, *Allen’s Astrophysical Quantities*, 4th edn. New York: AIP Press, Springer  
 de Vaucouleurs G., 1958, *AJ*, 63, 253  
 Diaferio A., Ramella M., Geller M. J., Ferrari A., 1993, *AJ*, 105, 6  
 Diaferio A., Geller M. J., Ramella M., 1994, *AJ*, 107, 3  
 Diaferio A., Kauffmann G., Colberg J. M., White S. D. M., 1999, *MNRAS*, 307, 537  
 Driver S. P., Allen P. D., Liske J., Graham A. W., 2007, *ApJ*, 657, L85  
 Eke V. R. et al., 2004, *MNRAS*, 348, 866  
 Ekholm T., Baryshev Y., Teerikorpi P., Hanski M., Paturel G., 2001, *A&A*, 368, L17  
 Frederic J. J., 1995a, *ApJS*, 97, 259  
 Frederic J. J., 1995b, *ApJS*, 97, 275  
 Geller M. J., Huchra J. P., 1983, *ApJS*, 52, 61  
 Gill S. P. D., Knebe A., Gibson B. K., 2004, *MNRAS*, 351, 399  
 Girardi M., Mezzetti M., Giuricin G., Mardirossian F., 1992, *ApJ*, 394, 442  
 Giudice G., 1999, *Properties of Nearby Groups of Galaxies*. Astron. Soc. Pac., San Francisco, p. 136  
 Giuricin G., Marinon C., Ceriani L., Pisani A., 2000, *ApJ*, 543, 178  
 Gott J. R. III, Turner E. L., 1977, *ApJ*, 213, 309  
 Gourgoulhon E., Chamaraux P., Fouqué P., 1992, *A&A*, 255, 69  
 Holmberg E., 1950, *Medd. Lunds Obs. Ser.*, 2, 128  
 Huchra J. P., Geller M. J., 1982, *ApJ*, 257, 423 (HG82)  
 Humason M. L., Mayall N. U., Sandage A. R., 1956, *ApJ*, 61, 97  
 Iovino A., Hickson P., 1997, *MNRAS*, 287, 21  
 Klypin A., Hoffman Y., Kravtsov A. V., Gottlöber S., 2003, *ApJ*, 596, 19  
 Knebe A., Green A., Binney J., 2001, *MNRAS*, 325, 845  
 Lahav O., Lilje P. B., Primack J. R., Rees M. J., 1991, *MNRAS*, 251, 128  
 Macció A. V., Governato F., Horellou C., 2005, *MNRAS*, 359, 941  
 Merchán M., Zandivarez A., 2002, *MNRAS*, 335, 216  
 Moore B., Frenk C. S., White S. D. M., 1993, *MNRAS*, 261, 827  
 Nolthenius R. A., White S. D. M., 1987, *MNRAS*, 235, 505  
 Nolthenius R., Klypin A. A., Primack J. R., 1997, *ApJ*, 480, 43  
 Oguri M., 2006, *MNRAS*, 367, 1241  
 Peirani S., de Freitas Pacheco J. A., 2006, *New Astron.*, 11, 325  
 Plionis M., Basilakos S., Ragone-Figueroa C., 2006, *ApJ*, 650, 770  
 Ramella M., Geller M. J., Huchra J. P., 1989, *ApJ*, 344, 57  
 Ramella M., Pisani A., Geller M. J., 1997, *AJ*, 113, 483  
 Ramella M., Geller M. J., Pisani A., da Costa L. N., 2002, *AJ*, 123, 2976  
 Sandage A., 1999, *ApJ*, 527, 479  
 Sandage A., Tammann G. A., 1975, *ApJ*, 196, 313  
 Schechter P., 1974, *ApJ*, 203, 557  
 Sulentic J., 1984, *ApJ*, 286, 542  
 Teerikorpi P., Chernin A. D., Baryshev Yu. V., 2005, *A&A*, 440, 791  
 Tucker D. L. et al., 2000, *ApJS*, 130, 237  
 Vale A., Ostriker J. P., 2004, *MNRAS*, 353, 189  
 Valtonen M. J., Byrd G. G., 1986, *ApJ*, 303, 523

This paper has been typeset from a  $\text{\TeX}/\text{\LaTeX}$  file prepared by the author.